Polarization in a Rashba strip coupled with a spiral spin density wave

2010 J. Phys.: Condens. Matter 22 215302

(http://iopscience.iop.org/0953-8984/22/21/215302)

J. Phys.: Condens. Matter **22** (2010) 215302 (6pp) doi:10.1088/0953-8984/22/21/215302

Polarization in a Rashba strip coupled with a spiral spin density wave

Zhi-Yong Zhang[1,2] **and Lang Chen**[2]

[1] Department of Physics, Nanjing University, Nanjing 210093, People's Republic of China
[2] School of Material Science and Engineering, Nanyang Technological University, 50 Nanyang Avenue, Singapore 639798, Singapore

E-mail: zyzhang@nju.edu.cn and langchen@ntu.edu.sg

Received 3 February 2010, in final form 29 March 2010
Published 5 May 2010
Online at stacks.iop.org/JPhysCM/22/215302

Abstract
The magnetoelectric effect in a Rashba strip is studied, which is coupled to a spiral spin density wave (SDW). The polarization, if it can be induced, must be perpendicular to the plane constructed by the helix axis and the wavevector of the SDW. With a gate voltage on the strip varied, the polarization fluctuates quickly and can be switched from a positive to a negative value or vice versa. Furthermore, reversing either the helix axis or the wavevector leads to the reversal of polarization. The main contributions to the polarization come from the eigenstates in the vicinity of the von Hove singularities. At half-filling, contributions from different eigenstates offset each other exactly. With the Rashba spin–orbit coupling increased, the averaged polarization displays an oscillatory behavior due to the spin precession, whereas with the exchange coupling increased, the averaged polarization increases first then decreases. Considering the size effect on the polarization, the spin precession length is an important characteristic length.

(Some figures in this article are in colour only in the electronic version)

1. Introduction

In the past decade, spintronics has made great progress with the hope of using spins, in addition to electrons or holes, for quantum information processing [1–3]. Due to the inversion asymmetry of the confining potential, the Rashba spin–orbit (SO) coupling [4] plays an important role in a two-dimensional electronic gas (2DEG) in semiconductor heterostructures. Although it may be erased by disorder in a bulk system, a pure spin current appears in the transverse direction—the so-called spin Hall effect (SHE)—with an unpolarized electronic current flowing through a mesoscopic Rashba system [5–8]. As a result, although the distribution of electrons is still symmetric, a nonequilibrium spin accumulation with opposite signs for the two lateral edges is induced [9]. This phenomenon demonstrates the coupling between spin and electric degrees of freedom in this type of system. An inverse question is, under the exchange coupling with magnetization, whether an 'electric' polarization can be formed in a mesoscopic Rashba system.

Recently, the interest in the magnetoelectric (ME) effect has been reignited because of the experimental discovery of multiferroics, e.g. $RMnO_3$ with R = Gd, Tb and Dy, the materials in which the magnetic and electric orders not only coexist but also are so strongly coupled that the magnetic degree of freedom can be manipulated by an electric field or vice versa [10–17]. For these multiferroic perovskites, the ME effect involves interplay between charge, spin, orbital and lattice degrees of freedom. Through symmetry analysis, Mostovoy showed that the ferroelectric order can be induced in spiral magnets, and that the helix axis, the wavevector of the spin density wave (SDW) and the polarization are perpendicular to each other and form a right-hand system [18]. Sergienko and Dagotto studied the influence of Dzyaloshinskii–Moriya (DM) interaction, an anisotropic exchange coming from spin–orbit coupling [19, 20], in multiferroic perovskites via a double-exchange model including the Jahn–Teller effect and found excellent agreement with experiments [21]. Some pure electronic mechanisms without the lattice degree of freedom have also been proposed to explain the polarization caused by the ME effect. Katsura *et al* proposed an inverse DM mechanism, in which the spin current induced between two noncollinear magnetizations leads to the electric polarization [22]. Hu suggested that in an unconventional insulator, e.g. a Mott insulator, with a strong SO coupling, noncollinear magnetism generates the ferroelectricity through an electric current cancellation process [23]. In these two models, the helix axis, the wavevector of the spiral SDW and the polarization also form a right-hand system.

In these pure electronic mechanisms, the spin–orbit coupling and noncollinear magnetizations are two crucial factors. Although they were oriented to explain the ME effect in multiferroic perovskites, the idea can be applied to other systems. In the present paper, we study the ME effect in a Rashba SO strip, which is coupled to a spiral SDW. The correlation between Rashba electrons and the SDW can be achieved via the proximity effect of a spiral magnet to the 2DEG. We expect the polarization can be formed in this Rashba strip if the spiral SDW takes an appropriate configuration. Our purpose is to clarify the characteristics of the ME effect under the Rashba SO coupling. Although it is realized that the SO coupling is necessary to the ME effect, the study on the characteristics of the specific SO coupling—the Rashba SO coupling—has not been performed. We find that the polarization, if it can be induced, must be perpendicular to the plane constructed by the helix axis and wavevector of the SDW. With a gate voltage on the strip varied, the polarization fluctuates quickly and can be switched from a positive to a negative value or vice versa. Furthermore, reversing either the helix axis or the wavevector leads to the reversal of polarization. The main contributions to the polarization come from the eigenstates in the vicinity of the von Hove singularities. At half-filling, contributions from different eigenstates offset each other exactly. With the Rashba SO coupling increased, the averaged polarization displays an oscillatory behavior due to the spin precession, whereas with the exchange coupling increased, the averaged polarization increases first then decreases. Considering the size effect on the polarization, the spin precession length is an important characteristic length.

The organization of this paper is as follows. In section 2, the theoretical model and the calculation method are presented. In section 3, the numerical results are presented and discussed. A brief summary is given in section 4.

2. Model and formulae

In our theoretical model, the corresponding Rashba strip is treated as a discrete lattice, which is L_W in width. (For simplicity, the lattice constant a_0 and the electronic charge e are set as unity except when the numerical results are compared with the experimental data.) The Rashba SO hopping parameter is t_{SO}. The correlation with a spiral SDW can be introduced in the strip via the proximity effect. The wavevector $\mathbf{Q}$ of the SDW is assumed to be along the longitudinal direction of the strip. The helix axis of the SDW can take three different directions: (I) it is perpendicular to the strip plane; (II) it is in the plane and perpendicular to $\mathbf{Q}$ and (III) it is parallel to $\mathbf{Q}$. That is, it is parallel to the z, y and x axes, respectively (cf figure 1, where a sketch of the system is given). For these three types of SDW, the magnetization at the lattice site $\mathbf{m} = m_x\mathbf{e}_x + m_y\mathbf{e}_y$ is

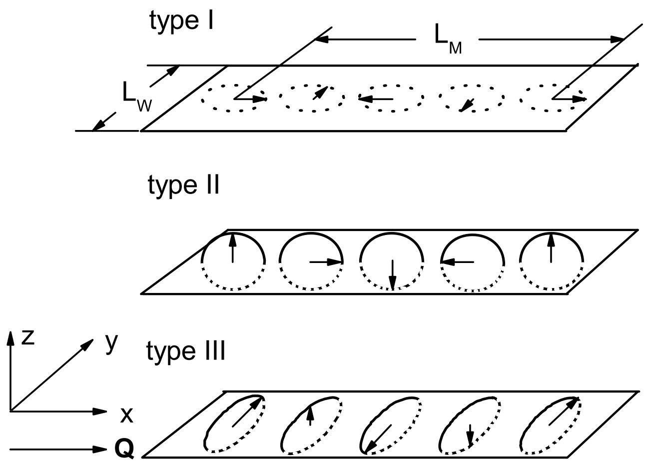

Figure 1. A sketch of the system.

$$\mathbf{M_m} = \begin{cases} M_0\cos(Qm_x)\mathbf{e}_x + M_0\sin(Qm_x)\mathbf{e}_y & \text{I} \\ M_0\cos(Qm_x)\mathbf{e}_z + M_0\sin(Qm_x)\mathbf{e}_x & \text{II} \\ M_0\cos(Qm_x)\mathbf{e}_y + M_0\sin(Qm_x)\mathbf{e}_z & \text{III.} \end{cases} \quad (1)$$

Here $\mathbf{e}_i$ with $i = x$, y and z are the unit basis vectors of Euclidean space. $\mathbf{Q} = Q\mathbf{e}_x = 2\pi/L_M\mathbf{e}_x$, and the SDW period L_M is assumed to be commensurate with the lattice. As a result, the strip structure displays a period of $L_N = qL_M$ with q an integer number. (L_N and q cannot have a common factor.) The magnetization is treated as a classic vector. At each lattice site, electrons couple to the corresponding magnetization via an exchange interaction.

Under these assumptions, the Hamiltonian of the system can be written in the tight-binding representation as [9]

$$H = \sum_{\mathbf{m}} \hat{c}^\dagger_{\mathbf{m}}\hat{S}_{\mathbf{m}}\hat{c}_{\mathbf{m}} + \sum_{\mathbf{mm}'} \hat{c}^\dagger_{\mathbf{m}}\hat{t}_{\mathbf{mm}'}\hat{c}_{\mathbf{m}'} \quad (2)$$

with $\hat{c}_{\mathbf{m}} = \binom{c_{\mathbf{m},\uparrow}}{c_{\mathbf{m},\downarrow}}$. $c^\dagger_{\mathbf{m},\sigma}$ ($c_{\mathbf{m},\sigma}$) is the creation (annihilation) operator of a spin σ electron at the site $\mathbf{m}$ with $\sigma =\uparrow$ or $\downarrow$. Due to the exchange interaction between electrons and magnetization, the generalized on-site energy $\hat{S}_{\mathbf{m}}$ is

$$-\hat{S}_{\mathbf{m}}/J = \begin{cases} \cos(Qm_x)\hat{\sigma}_x + \sin(Qm_x)\hat{\sigma}_y & \text{I} \\ \cos(Qm_x)\hat{\sigma}_z + \sin(Qm_x)\hat{\sigma}_x & \text{II} \\ \cos(Qm_x)\hat{\sigma}_y + \sin(Qm_x)\hat{\sigma}_z & \text{III} \end{cases} \quad (3)$$

where $\hat{\sigma}_i$ with $i = x$, y and z are the Pauli matrices. Taking the Rashba coupling into account, the generalized nearest-neighbor hopping integral is

$$\hat{t}_{\mathbf{mm}'} = \begin{cases} -t_0\hat{1} - \mathrm{i}t_{SO}\hat{\sigma}_y & \mathbf{m} = \mathbf{m}' + \mathbf{e}_x \\ -t_0\hat{1} + \mathrm{i}t_{SO}\hat{\sigma}_x & \mathbf{m} = \mathbf{m}' + \mathbf{e}_y \end{cases} \quad (4)$$

where $\hat{1}$ is a 2×2 unit matrix. In this Rashba strip of a discrete lattice, the spin precession length [9], on which a spin precesses by an angle π, is $L_{SO} = \pi t_0/(2t_{SO})$.

The single-electron wavefunction can be written as

$$\Psi = \sum_{\mathbf{m},\sigma} a_{\mathbf{m},\sigma} c^{\dagger}_{\mathbf{m},\sigma} |0\rangle. \quad (5)$$

From the Bloch theorem, it is known that $a_{\mathbf{m}+L_N \mathbf{e}_x,\sigma} = e^{ikL_N} a_{\mathbf{m},\sigma}$ with $0 \leqslant k < 2\pi/L_N$. For each k, the Hamiltonian equation (2) can be diagonalized within a unit cell which is L_N in length and L_W in width. This results in $2L_N L_W$ eigenenergies $E_\alpha(k)$ and corresponding $2L_N L_W$ eigenfunctions $\Psi_\alpha(k)$. Because of the periodicity in the longitudinal direction and because of the two-dimensional nature of the Rashba strip, a net polarization, if it can be formed, can only be found in the transverse direction. For the eigenfunction $\Psi_\alpha(k)$, the polarization averaged in a unit cell is

$$P_\alpha(k) = \frac{1}{L_N L_W} \sum_{m_x=1}^{L_N} \sum_{m_y=1}^{L_W} \sum_{\sigma} \left(m_y - \frac{L_W+1}{2} \right) |a_{\mathbf{m},\sigma}|^2. \quad (6)$$

Here, $a_{\mathbf{m},\sigma}$ is also a function of α and k, but for clarity, these two indexes are not written explicitly. In the above equation, if $\sum_\sigma |a_{\mathbf{m},\sigma}|^2$ is replaced by $\hat{a}^{\dagger}_{\mathbf{m}} \hat{\sigma}_i \hat{a}_{\mathbf{m}}$, the spin polarization can be calculated. But in the present paper, our attention is focused on the 'electric' polarization in this Rashba strip. At zero temperature, electrons occupy those eigenstates one by one from the lowest level until the Fermi energy E_F. The total polarization is

$$P(E_F) = \frac{L_N}{2\pi} \sum_{E_\alpha \leqslant E_F} \int_{k=0}^{2\pi/L_N} P_\alpha(k)\, dk. \quad (7)$$

In this Rashba strip, the particle–hole symmetry with respect to $E_F = 0$ is reserved, and only the occupation ratio less than half-filling needs to be studied.

3. Results and discussion

Our numerical results show that if the electrons in the Rashba strip couple to the SDW of types II and III, no net polarization can be formed in the transverse direction. Only when the strip couples to the SDW of type I can net polarization be found. This is consistent with the conclusion of the previous theoretical works on multiferroic perovskites that the ME-effect-induced polarization must be perpendicular to both the helix axis and the wavevector of the spiral SDW [18, 21–23]. Below, we only consider the results of type I.

The variation of P with E_F is plotted for $t_{SO}/t_0 = J/t_0 = 0.1$ and 0.2 in figures 2(a) and (b), respectively. As E_F varied, P fluctuates quickly and can take both positive and negative values. Since the Fermi energy can be varied by adjusting a gate voltage on the 2DEG, that means the polarization of the Rashba strip can be reversed from along the y axis to opposite to it or vice versa by changing an external voltage. In this reversing process, the magnitude of polarization is also changed. With E_F fixed, changing t_{SO} and/or J can also realize that type of reversing. For example, at $E_F/t_0 = -0.07$, when $t_{SO}/t_0 = J/t_0 = 0.1$, $P = 0.195$, and when $t_{SO}/t_0 = J/t_0 = 0.2$, $P = -0.0297$. These results are contrary to the previous

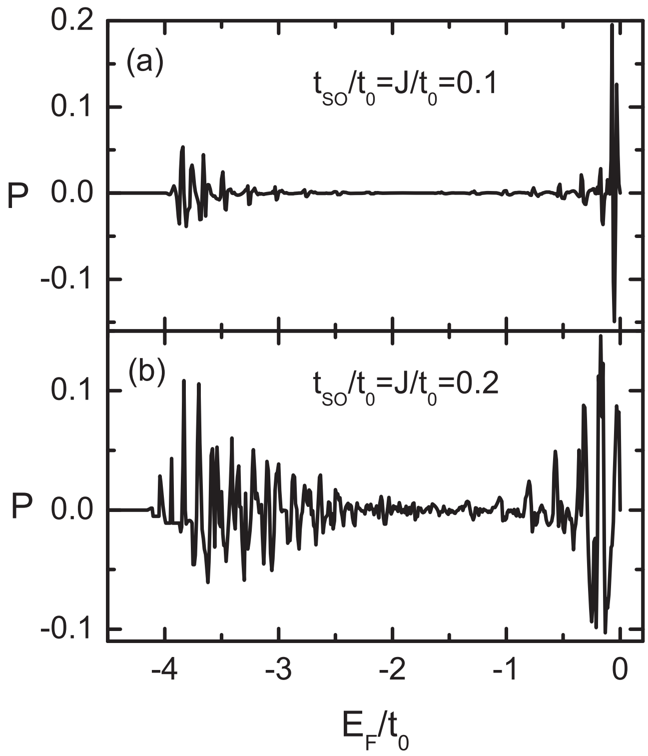

Figure 2. P–E_F curves with (a) $t_{SO}/t_0 = J/t_0 = 0.1$ and (b) $t_{SO}/t_0 = J/t_0 = 0.2$ for $L_N = L_M = 10$ and $L_W = 20$.

theoretical works on multiferroic perovskites, which predict that the helix axis, wavevector $\mathbf{Q}$ and polarization can only form a right-hand system [18, 21–23], whereas in our model, both a right-hand and a left-hand systems can be formed.

However, at a specific parameter point (E_F, t_{SO}, J), which one of the two systems can be formed is determined. With the helix axis or the wavevector reversed, the polarization is also reversed. For example, we have also calculated the P–E_F curves for $q \neq 1$ and the same characteristics as $q = 1$ can be found, but the polarizations of the two structures corresponding to $L_M = L_N/q$ and $L'_M = L_N/(L_N - q)$ have the same amplitude but point to the opposite directions. This is because $Q' = 2\pi/L'_M = -2\pi q/L_N (\mathrm{mod}\ 2\pi) = -Q$, or in other words, the wavevector is reversed.

Figure 2 is obtained with $L_W = 20$. To observe the variation of P with E_F more clearly, the P–E_F curves and the corresponding density of states (DOS) for $L_W = 4$ are given in figures 3(a) and (b) with $t_{SO}/t_0 = J/t_0 = 0.1$ and 0.2, respectively. As a comparison, the results for $L_W = 8$ with $t_{SO}/t_0 = J/t_0 = 0.1$ are given in figure 3(c). At $t_{SO} = J = 0$, there are L_W spin-degenerate channels in the transverse direction, and the DOS shows L_W von Hove singularities in the range $E_F < 0$. With t_{SO} and J increased from zero, the number of von Hove singularities increases since there are $2L_N L_W$ transverse channels now. These singularities can be divided into L_W groups, corresponding to the L_W 'old' singularities. In the same positions as these groups except the lowest one, the amplitude of P fluctuation is much larger than that away from the groups, which means that the main contribution to the polarization is given by the eigenstates with group velocity $v_g \sim 0$. However, in the lowest group, the amplitude is

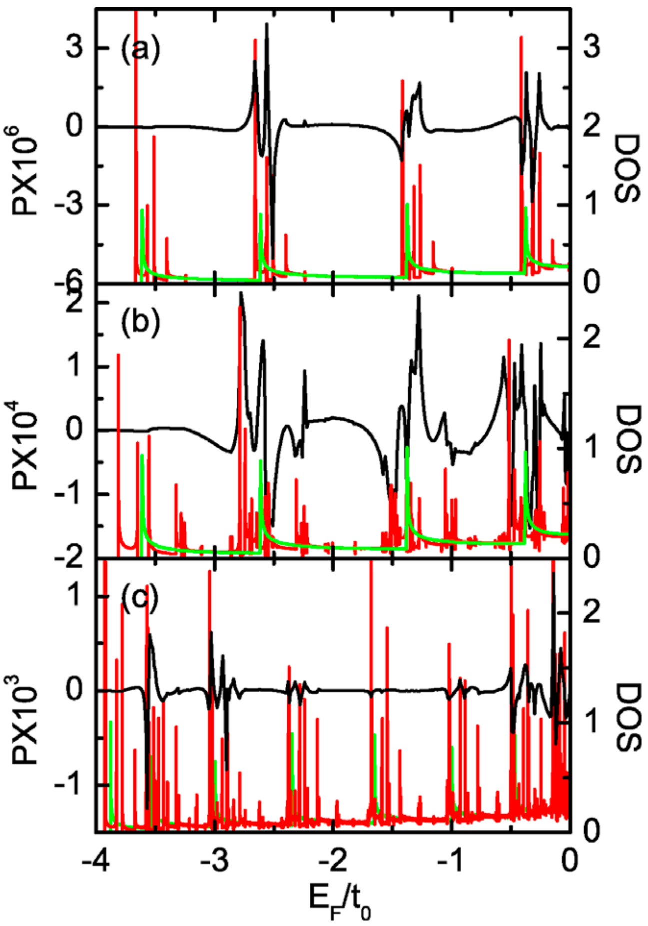

Figure 3. P–E_F (black) and DOS (red or dark grey) curves with (a) $t_{SO}/t_0 = J/t_0 = 0.1$ and $L_W = 4$, (b) $t_{SO}/t_0 = J/t_0 = 0.2$ and $L_W = 4$, and (c) $t_{SO}/t_0 = J/t_0 = 0.1$ and $L_W = 8$ for $L_N = L_M = 10$. The DOS curves for $t_{SO}/t_0 = J/t_0 = 0$ (green or light grey) are also plotted in the corresponding diagrams.

small (but not zero). Since at $t_{SO} = J = 0$, the lowest singularity corresponds to a single spin-degenerate channel, this contrast demonstrates the importance of hybridization between different spin-degenerate channels to the formation of polarization.

Carefully checking the numerical data shows that the contribution of an individual eigenstate to the polarization can be positive or negative. At half-filling, although there are more eigenstates contributing to the polarization than the other occupation ratios, the polarization is zero, or in other words, those contributions offset each other exactly. This characteristic is different from that of Hu's model, in which the system must be an unconventional insulator, e.g. a Mott insulator at half-filling, to guarantee an electric current cancellation process [23].

From figure 3, one can see that, when t_{SO} and J take small non-zero values, corresponding to the groups in the middle of the lower half-band, the amplitude is much smaller than that in the groups close to the band center and the band bottom. With t_{SO} and J increased, two types of variation trends can be found. First, the ranges of every singularity groups are expanded. And, second, the amplitude difference between different groups becomes smaller. (Similar trends can also be found in figure 2.) For $L_W = 4$, with $t_{SO}/t_0 = J/t_0$ increased from 0.1 to 0.2, the maximum amplitude is increased from $\sim 10^{-6}$ to $\sim 10^{-4}$. For $t_{SO}/t_0 = J/t_0 = 0.1$ with L_W increased from 4 to 8, that value can reach to $\sim 10^{-3}$. However, in figure 2, for $L_W = 20$, with $t_{SO}/t_0 = J/t_0$ increased from 0.1 to 0.2, the maximum amplitude ~ 0.1 is almost unchanged.

Below, we are going to further clarify how the size effect, and the Rashba SO and exchange couplings, affect the polarization. Since P fluctuates with E_F quickly, to simplify the analyzing, an averaged polarization is defined:

$$\langle P^2 \rangle^{\frac{1}{2}} = \sqrt{-\frac{1}{E_B}\int_{E_B}^{0} |P(E_F)|^2 \, dE_F}. \tag{8}$$

Here, E_B is the band bottom, which is related to structural parameters, and t_{SO} and J.

The variations of the averaged polarization with t_{SO} and J are illustrated in figures 4(a) and (b), respectively. These results are obtained for $L_N = L_M = 10$ and $L_W = 20$. If either of the two couplings, t_{SO} and J, disappears, the polarization is zero. This fact confirms that, in this structure, the interplay of the Rashba SO and the exchange couplings plays a crucial role in the ME effect. With fixed $J \neq 0$, when t_{SO} is increased from zero, the averaged polarization increases first. As t_{SO} increased further with $2L_{SO} < L_W$, it displays an oscillatory behavior, and in this process the oscillation is still upward. On the other hand, with fixed $t_{SO} \neq 0$, when J is increased from zero, the averaged polarization increases first and reaches to a maximum point. Then it decreases with J. The position of the maximum point is related to t_{SO}/t_0. For $t_{SO}/t_0 = 0.2$, it should take a larger J to reach to that point than for $t_{SO}/t_0 = 0.1$.

To clarify the size effect on the polarization in this Rashba strip, the $\langle P^2 \rangle^{\frac{1}{2}}$–$L_W$ curves for $L_N = L_M = 10$ at $t_{SO}/t = J/t = 0.1$ and 0.2 are given in figure 5. The polarization is zero when $L_W < 4$. The threshold value is independent with t_{SO} and J, and this phenomenon further demonstrates the importance of hybridization between different spin-degenerate channels. With L_W increased from 4, the averaged polarization appears and increases. Then, it oscillates with L_W. With L_W larger than $2L_{SO}$, although the averaged polarization still oscillates with L_W, the general trend of the oscillation becomes stable. Here, $L_{SO} = 15.7$ at $t_{SO}/t = 0.1$, and 7.86 at $t_{SO}/t = 0.2$.

In figure 6, the $\langle P^2 \rangle^{\frac{1}{2}}$–$L_N$ curves are presented for $L_W = 20$ at $t_{SO}/t = J/t = 0.1$ and 0.2. These results are obtained with $q = 1$. At $L_N = 2$, $\langle P^2 \rangle^{\frac{1}{2}}$ is zero since the spiral SDW reduces to an anti-ferromagnetic arrangement in the longitudinal direction of the strip. With L_N increased from 2, the averaged polarization appears and increases. With L_N increased further, for $t_{SO}/t = J/t = 0.1$, no obvious oscillatory behavior can be found, whereas for $t_{SO}/t = J/t = 0.2$, $\langle P^2 \rangle^{\frac{1}{2}}$ displays an oscillatory behavior. This is because, for the former, $2L_{SO} > L_W$, whereas for the latter, $2L_{SO} < L_W$. However, no matter whether the curves display an oscillatory behavior or not, the variation trend of $\langle P^2 \rangle^{\frac{1}{2}}$ becomes stable for large L_N since at this time the magnetization of the spiral SDW varies adiabatically. In this

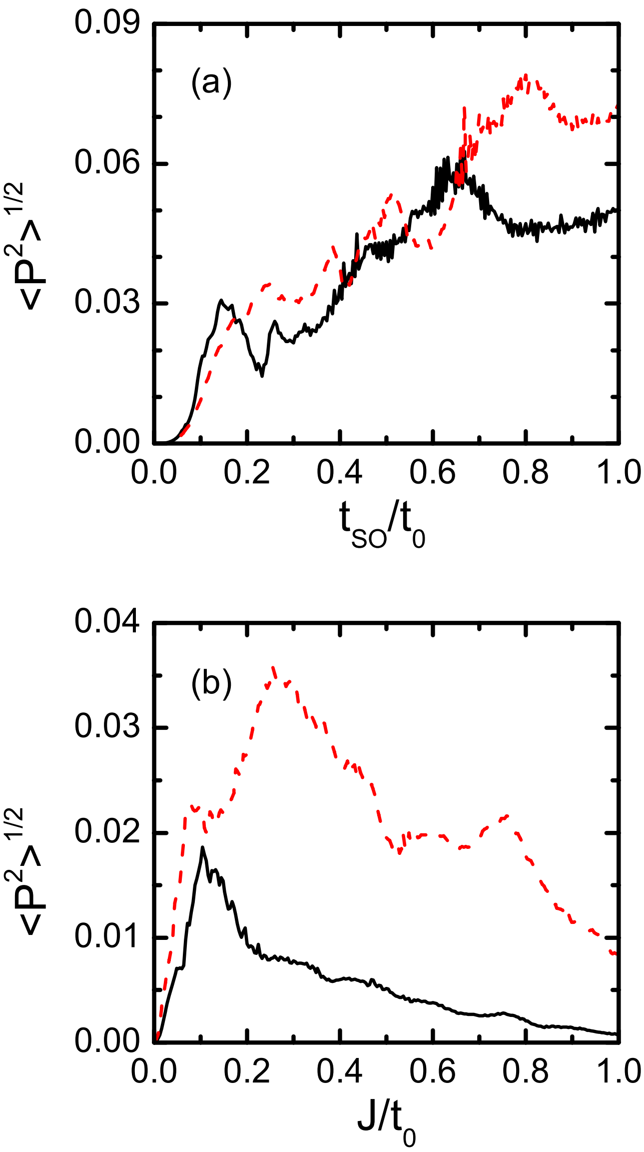

Figure 4. (a) $\langle P^2\rangle^{\frac{1}{2}}$–$t_{SO}$ curves with $J/t_0 = 0.1$ (black solid) and 0.2 (red dashed). (b) $\langle P^2\rangle^{\frac{1}{2}}$–$J$ curves with $t_{SO}/t_0 = 0.1$ (black solid) and 0.2 (red dashed). The other parameters are the same as in figure 2.

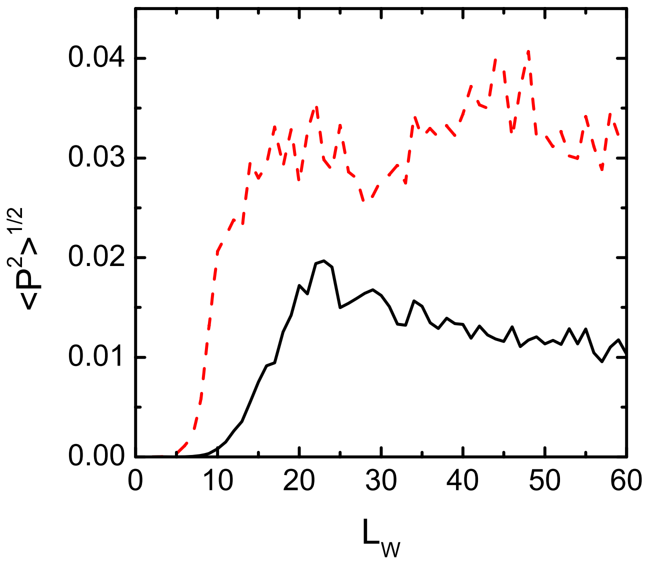

Figure 5. $\langle P^2\rangle^{\frac{1}{2}}$–$L_W$ curves with $t_{SO}/t_0 = J/t_0 = 0.1$ (black solid) and 0.2 (red dashed) for $L_N = L_M = 10$.

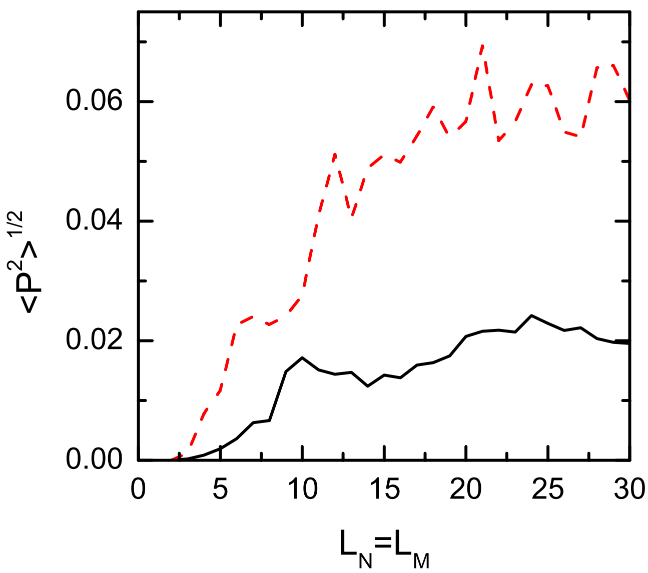

Figure 6. $\langle P^2\rangle^{\frac{1}{2}}$–$L_N$ curves with $t_{SO}/t_0 = J/t_0 = 0.1$ (black solid) and 0.2 (red dashed) for $L_N = L_M$ and $L_W = 20$.

situation, the period of every two oscillatory peaks is about L_{SO} for $t_{SO}/t = J/t = 0.2$.

In the above calculations, P is obtained even for $t_{SO}/t_0 = 1$ to give an overall picture of the polarization. But in experiments, such large t_{SO}/t_0 cannot be reached. In fact, in the tight-binding Hamiltonian (2), t_0 and t_{SO} are related with the effective electron mass m^*, the Rashba coupling strength α_R and the lattice constant a_0 as [9] $t_0 = \hbar^2/(2m^*a_0^2)$ and $t_{SO} = \alpha_R/(2a_0)$. With a_0 and m^* taken as 3 nm and $0.041m_e$, t_0 is 103 meV. At $t_{SO}/t_0 = J/t_0 = 0.1$, the corresponding α_R is about 61.9 meV nm, which is available in experiments [24, 25]. With these parameters, $\langle P^2\rangle^{\frac{1}{2}}$ can reach to 0.02 (cf figure 6). Consequently, the averaged polarization is $\sim 1.07\times10^{-8}$ μC cm^{-1}, which is strong enough to be detected experimentally. At some occupation ratios, the polarization can even be one order of magnitude larger than the averaged one. Of course, the rapid fluctuation of P becomes smooth when a finite temperature is introduced. But only if $k_BT < \min[t_{SO}, J]$, the interplay between the Rashba SO interaction and the exchange coupling leads to the polarization. The threshold temperature is about 120 K.

All of these results are obtained under the assumption of translational invariance, but the imperfection—e.g. impurities, localized Rashba interactions, etc—is inevitable in the process of sample fabrication, which leads to the failure of the Bloch theorem. The present fabrication technique can control the impurity density to such a degree that the coherence length is long enough. In this Rashba strip, the polarization originates from the subtle spin precession of electrons under the coupling with an external spiral SDW. However, the localized Rashba interaction can cause spin decoherence. Of course, the influence of spin decoherence on this type of 'electric' polarization is an interesting topic for later work. But only if this effect is not so strong should the polarization be observable.

4. Summary

In summary, we have studied the ME effect in a Rashba strip, which is coupled to a spiral SDW. The polarization, if it can be induced, must be perpendicular to both the helix axis and the wavevector of the SDW. With a gate voltage on the 2DEG varied, P fluctuates quickly and can be switched from a positive to a negative value or vice versa. Furthermore, reversing either the helix axis or the wavevector leads to the reversal of P. The main contributions to the polarization come from the eigenstates in the vicinity of the von Hove singularities. At half-filling, contributions from different eigenstates offset each other exactly. With t_{SO} increased, the averaged polarization displays an oscillatory behavior due to the spin precession, whereas with J increased, it increases first then decreases. Considering the size effect on the polarization, the spin precession length is an important characteristic length.

Acknowledgments

We acknowledge the support from Nanyang Technological University under grant no. SUG 13/06 and MoE Tier1 RG 21/07. Z-YZ acknowledges the Natural Science Foundation of Jiangsu Province, China under grant no. BK2009224.

References

[1] Prinz G A 1998 *Science* **282** 1660
[2] Awschalom D, Loss D and Samarth N (ed) 2002 *Semiconductor Spintronics and Quantum Computation* (Berlin: Springer)
[3] Zutic I, Fabian J and Das Sarma S 2004 *Rev. Mod. Phys.* **76** 323
[4] Rashba E I 1960 *Fiz. Tverd. Tela* **2** 1224
Rashba E I 1960 *Sov. Phys.—Solid State* **2** 1109 (Engl. Transl.)
[5] Murakami S, Nagaosa N and Zhang S-C 2003 *Science* **301** 1348
Murakami S, Nagaosa N and Zhang S-C 2004 *Phys. Rev.* B **69** 235206
[6] Sinova J, Culcer D, Niu Q, Sinitsyn N A, Jungwirth T and MacDonald A H 2004 *Phys. Rev. Lett.* **92** 126603
[7] Shen S-Q 2005 *Phys. Rev. Lett.* **95** 187203
[8] Nikolic B K, Zarbo L P and Welack S 2005 *Phys. Rev.* B **72** 075335
[9] Nikolic B K, Souma S, Zarbo L P and Sinova J 2005 *Phys. Rev. Lett.* **95** 046601
[10] Tokura Y 2006 *Science* **312** 1481
[11] Cheong S W and Mostovoy M 2007 *Nat. Mater.* **6** 13
[12] Kimura T, Goto T, Shintani H, Ishizaka K, Arima T and Tokura Y 2003 *Nature* **426** 55
[13] Hur N, Park S, Sharma P A, Ahn J S, Guha S and Cheong S W 2004 *Nature* **429** 392
[14] Hur N, Park S, Sharma P A, Guha S and Cheong S W 2004 *Phys. Rev. Lett.* **93** 107207
[15] Chapon L C, Blake G R, Gutmann M J, Park S, Hur N, Radaelli P G and Cheong S W 2004 *Phys. Rev. Lett.* **93** 177402
[16] Goto T, Kimura T, Lawes G, Ramirez A P and Tokura Y 2004 *Phys. Rev. Lett.* **92** 257201
[17] Kimura T, Lawes G and Ramirez A P 2005 *Phys. Rev. Lett.* **94** 137201
[18] Mostovoy M 2006 *Phys. Rev. Lett.* **96** 067601
[19] Dzyaloshinskii I 1958 *J. Phys. Chem. Solids* **4** 241
[20] Moriya T 1960 *Phys. Rev.* **120** 91
[21] Sergienko I A and Dagotto E 2006 *Phys. Rev.* B **73** 094434
[22] Katsura H, Nagaosa N and Balatsky A V 2005 *Phys. Rev. Lett.* **95** 057205
[23] Hu J 2008 *Phys. Rev. Lett.* **100** 077202
[24] Nitta J, Akazaki T, Takayanagi H and Enoki T 1997 *Phys. Rev. Lett.* **78** 1335
[25] Cui L J, Zeng Y P, Wang B Q, Zhu Z P, Lin L Y, Jiang C P, Guo S L and Chu J H 2002 *Appl. Phys. Lett.* **80** 3132